Supplemental Information for "Loss of Smooth Muscle α-actin Leads to NF-κB-Dependent Increased Sensitivity to Angiontensin II in Smooth Muscle Cells and Aortic Enlargement"

Supplemental Methods

2D gel electrophoresis and mass spectrometry analyses

Cultured SMCs or freshly isolated ascending aortic tissue were homogenized in urea sample buffer, containing 8M urea, 20mM Tris, 23mM glycine, 0.2mM EDTA, 5% saturated sucrose, and 10mM DTT. Three micrograms of cell lysates mixed with or without 200ng of purified SM α-actin or SM γ-actin (provided by Dr. Kathleen Trybus from the University of Vermont) were added into 450μL of Rehydration/Sample buffer (Bio-Rad). Samples were loaded onto 24 cm, pH 4–7, immobilized pH gradient strips (Bio-Rad) overnight and focused in a PROTEAN® i12™ IEF System (Bio-Rad) for 60kVh. Then, the strips were equilibrated in Equilibration Buffer I and II (Bio-Rad), the center third parts were cut out and saved, and the strips were gently inserted into a 8-12% SDS-PAGE mini-gel (Bio-Rad). Then, the gel was run, transferred to nitrocellulose membrane, blotted with anti-pan actin antibody (MA5-11869, Sigma), and visualized as described in routine immunoblotting. The calculated isoelectric points for α-, β-, and γ-actin are 5.24, 5.29, and 5.31, respectively. For mass spectrometry analysis, gels were minimally stained with Coomassie brilliant blue. Bands of interest were cut out, proteins eluted, and subjected to trypsin digestion. The tryptic digests were analyzed by mass spectrometry.

Blood pressure measurements: noninvasive Tail-Cuff method

The VPR noninvasive blood pressure monitoring system (CODA^{TM}, Kent Scientific Corporation, CT) was used to measure blood pressures. Mice were conditioned to the restraint

and warming chamber for 20 min/day for at least 3 days. After 5–10 min of stabilization in the chamber, mice were subjected to automated inflation-deflation cycles at 1 cycle/minute for 40 minutes. Pressures were measured on three successive days; the first day's measurements were discarded. We examined each cycle and discarded obviously aberrant tracings due to movement or artifacts. Systolic pressure for each usable cycle was averaged to generate a single systolic value for each mouse (minimum 40 cycles per mouse). Blood pressure was measured at 2 months of age on at least 6 mice per group.

Mouse Echocardiography

We performed transthoracic echocardiography on age matched WT and *Acta2*$^{-/-}$ littermates to determine aortic diameter *in vivo*. Two-dimensional and M-mode echocardiography images were recorded and analyzed using a Vevo 770 equipped with a 40 MHz ultrasonic linear probe (VisualSonics, Toronto, Ontario, Canada). Images were obtained in the parasternal long-axis view. Aortic diameter measurements were made in late diastole.

Aortic Histopathology

Mice were anesthetized using 2.5% avertin, and aortas were perfused with normal saline followed by 10% neutral-buffered formalin at physiologic pressure, fixed, and paraffin-embedded. Aortic tissues were stained with H&E, MOVAT, or specific antibodies (**Supplemental table I**) according to standard protocols. Specimens were imaged using an Olympus microscope. All quantifications were performed using ImageJ (NIH). Cell density and elastin breaks were quantified using the cell counter function. % proteoglycans was quantified from MOVAT by a thresholding mechanism to count pixels that were blue (proteoglycans). All quantitative analyses were performed by two or more researchers.

Electron Microscopy

Mice were perfused with PBS, followed by 3% glutaraldehyde in 0.1% sodium cacodylate (pH=7.4) to fix the tissues. Aortas were dissected out and fixed further overnight, then treated sequentially with osmium tetroxide, tannic acid and uranyl acetate and dehydrated and embedded in Epon as previously described (1). Sixty-nanometer sections were counterstained with 7% methanolic uranyl acetate and lead citrate and observed using Tecnai 12 transmission electron microscope operating at 120 kV.

Measurement of ROS in aortas by DHE staining

Descending aortas were harvested, rinsed immediately in cold PBS, placed in Tissue-Tek OCT compound (Miles Laboratories), and snap frozen in liquid nitrogen. Blocks were cut to 30 μm-thick cryosections on a cryostat. Frozen sections were fixed in 4% PFA at room temperature for 15 minutes and rinsed 3x with PBS. DHE (Invitrogen, Cat#C10422) stock at 2.5 mM was diluted for a final concentration of 10 μM in PBS and applied to each tissue section. Slides were incubated in a light-protected humidified incubator at 37°C for 30 minutes. DHE was counterstained with DAPI. Sections were imaged within 8 hours of staining with a fluorescent ZEISS AXIOSKOP 40 microscope. Identical acquisition settings were used for tissue from wild-type or mutant animals. Fluorescence images were quantified with ImageJ. Integrated fluorescence intensity (IFI) was calculated by integrating the area and strength of red staining within the aortic wall in each image. Error bars represent standard error.

NADPH Oxidase Activity Assay.

Aortic tissues harvested from 2 months old mice (n=4 per group) were ground in chilled grinding vials and were homogenized in lysis buffer (20 mmol/l KH_2PO_4, 1 mmol/l EGTA, and protease inhibitors cocktail; pH 7.4) and sonicated for 5s (3x with 10s interval). The homogenates were then centrifuged at 750 *g* for 5 min. The pellet was discarded and the supernatant was collected and subjected to a lucigenin-enhanced luminescence assay as described before (32) to determine NADPH oxidase activity in the aortic tissue homogenate. Protein content was measured in an aliquot of homogenate by Bradford assay.

NADPH oxidase activity was measured by chemiluminescence in a well containing assay phosphate buffer (50 mM KH_2PO_4, 1 mM EGTA, and 150 mM sucrose; pH 7.4), 5 μM lucigenin (Sigma), and the sample (50 μl). Reactions (final volume, 250 μl) were initiated by addition of 100 μM NADPH (Sigma). Luminescence was measured every second for 5 min in a luminometer (BioTek Synergy™ HT; BioTek Instruments, Inc., Winooski, VT). A background value was subtracted from each reading. Activity was calculated from the ratio of mean light units to total protein level and expressed as arbitrary units (relative light unit).

Calcium imaging

Cells were seeded on 25mm coverslips and pretreated with the indicated drugs for the indicated times. Cells were loaded with Fura-2AM for 10-15 minutes and then placed in the imaging chamber with 0.5mL of culture medium. Coverslips were mounted for viewing on a Nikon TE200 microscope, and imaging was performed with Incytim2 software (Intracellular Imaging, Inc.). Measurements were taken using excitation wavelengths of 343/380 nm and emission wavelength of 520 nm. Basal Ca^{++} was assessed for 20 seconds, then 0.5mL of medium containing the indicated amounts of AngII was added to the chamber. Imaging continued until Ca^{++} levels returned to baseline. Data is represented as Fmax/F0 where Fmax represents the highest 340/380 ratio and F0 represents the baseline 340/380 ratio for each cell.

αSKA-fp and αSMA-fp peptide experiments

Wild-type SMCs were seeded and allowed to settle overnight. The cells were serum-starved 24hr in 1% SmBM then treated with 10ng/mL TGF-β1 for 48hr. Then, cells were incubated with 1ug/mL of either αSKA-fp or αSMA-fp peptides for 24 hours in Owens media. Both peptides have been previously characterized (2).

Flow cytometry

Cells were trypsinized and labeled with Mitosox red (5μM) for 30 minutes. Probes were washed out using PBS, and cells were resuspended in PBS for reading on a flow cytometer. Data were analyzed using CellQuest Pro and Kaluza software.

References

(1) Davis EC. Smooth muscle cell to elastic lamina connections in developing mouse aorta. Role in aortic medial organization. *Lab Invest* 1993;68:89-99.

(2) Hinz B, Gabbiani G, Chaponnier C. The NH2-terminal peptide of alpha-smooth muscle actin inhibits force generation by the myofibroblast in vitro and in vivo. *J Cell Biol* 2002;157:657-63.

Online Figures and Figure Legends

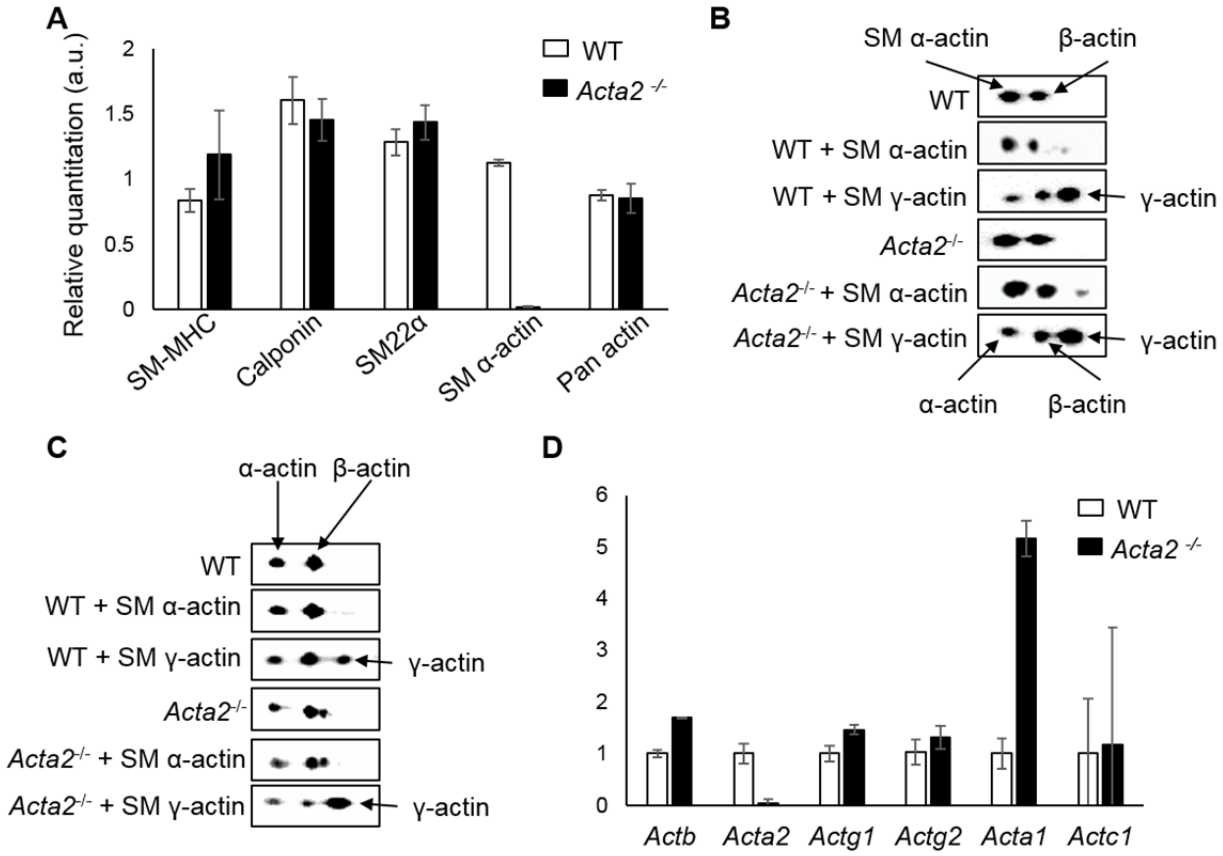

Online Figure I Expression of contractile proteins in *Acta2*$^{-/-}$ aortas (A) Quantitation of immunoblot shown in Figure 1C shows no change in expression of SM-MHC, Calponin, SM22α or total actin in *Acta2-/-* aortas compared with WT. Results are normalized to Gapdh. (B,C) Lysates of WT and *Acta2*$^{-/-}$ mouse aortic SMCs (B) or aortic tissue (C) were separated by two-dimensional gel electrophoresis and blotted with anti-pan actin antibody. SM α-actin and β-actin are found in WT cell lysates, while there are also two bands in *Acta2*$^{-/-}$ cell lysates. When purified SM α-actin was added into the cell lysates, the first band (α-actin)was enhanced in both genotypes. A third band appears in both genotypes after mixing the lysates with purified SM γ-actin, indicating another isoform of α-actin (skeletal or cardiac) compensates in *Acta2*$^{-/-}$ SMCs. (D) Quantitative PCR confirms that the compensating isoform is *Acta1* (skeletal α-actin).

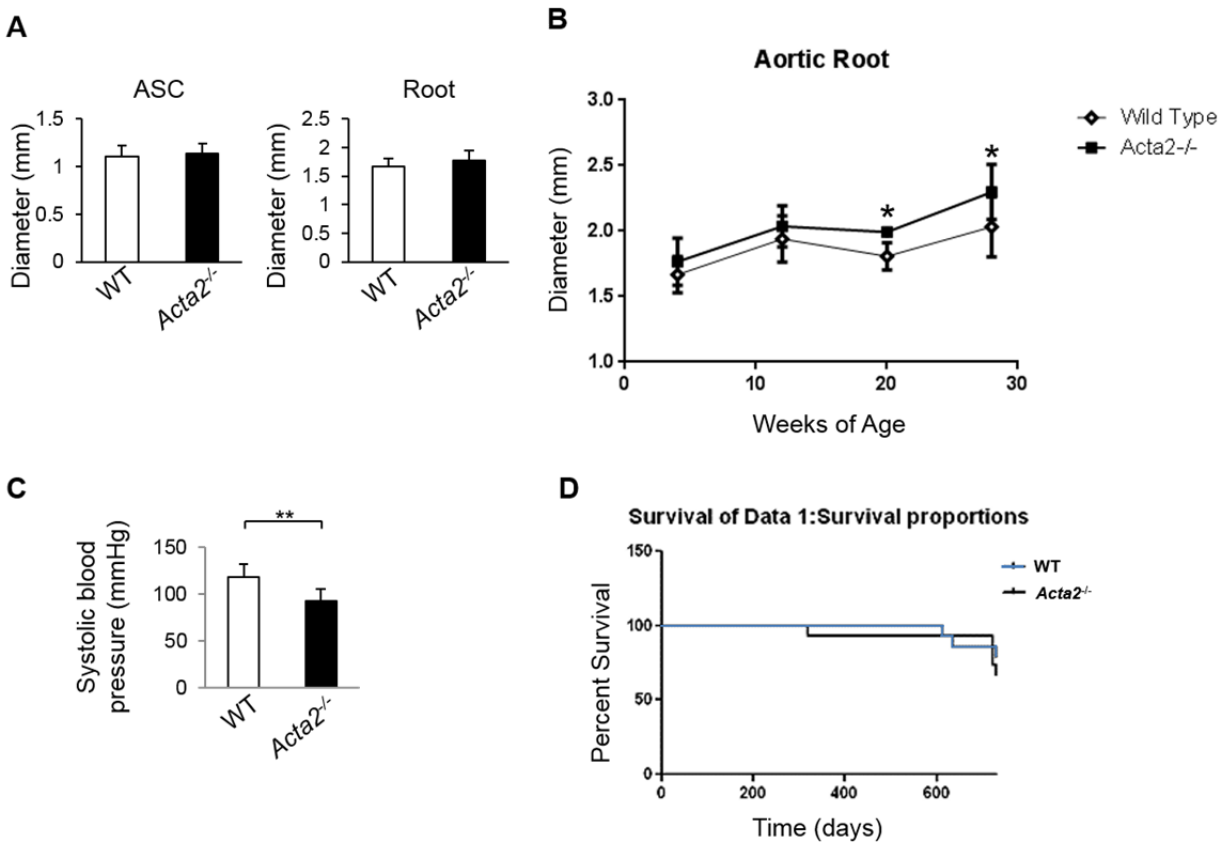

Online Figure II Aortic enlargement over time in *Acta2*$^{-/-}$ mice does not lead to dissection

(A) Echocardiography shows no enlargement of the ascending aorta or aortic root in *Acta2*$^{-/-}$ mice at 4 weeks of age. (B) Longitudinal studies with echocardiograms performed at 4, 12, 20, and 28 weeks of age show progressive aortic root dilation in *Acta2*$^{-/-}$ mice, which becomes significant at 18 weeks of age. (C) Tail cuff blood pressure measurements show decreased systolic blood pressure in *Acta2*$^{-/-}$ mice (n=6 mice per genotype). (D) There is no significant difference in the lifespan of *Acta2*$^{-/-}$ mice compared with controls, suggesting the observed dilation does not progress to aortic dissection (p=0.72 by Mantel-Cox analysis, n=15 mice per genotype).

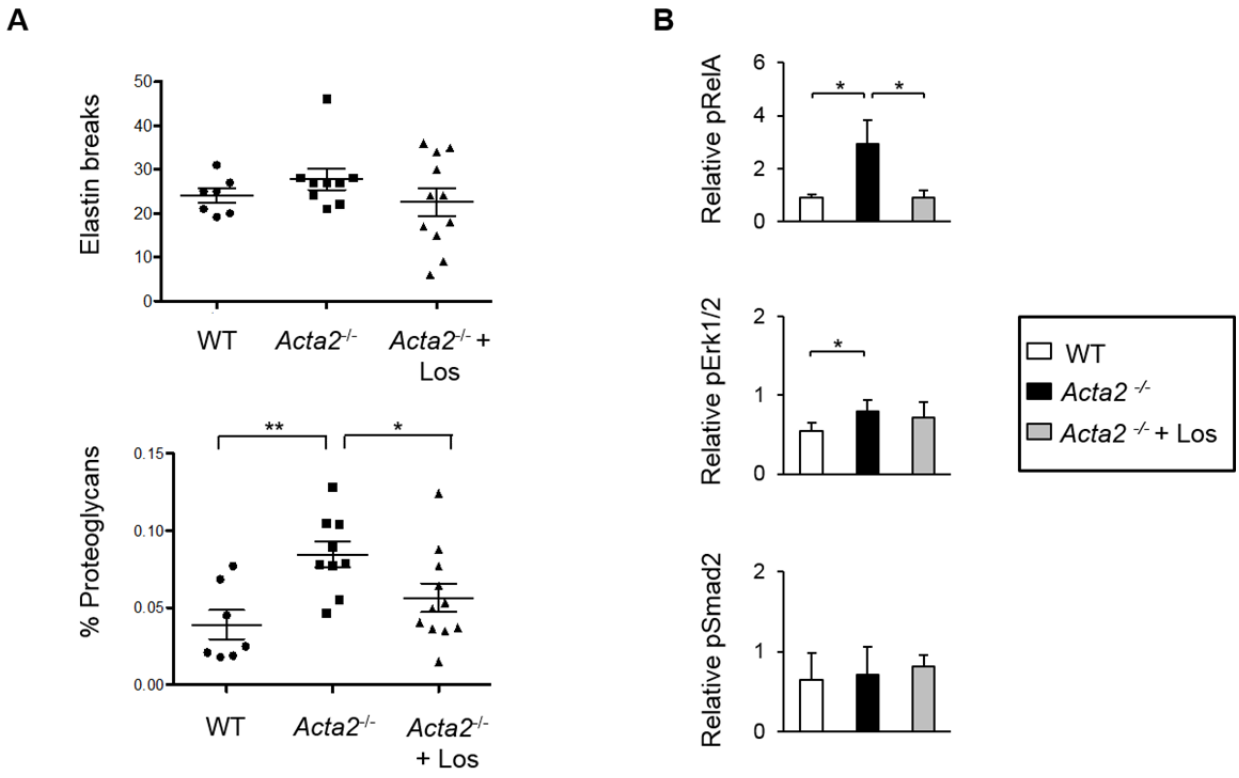

Online Figure III Mild medial degeneration and pathologic signaling changes in *Acta2*$^{-/-}$ aortas (A) Quantification of histologic changes in *Acta2*$^{-/-}$ aortas shows increased deposition of proteoglycans which is attenuated with losartan treatment, but no changes in elastin fragmentation (n=7 or more per group). (B) Quantification of blots shown in Figure 2G shows increased pRelA and increased pERK1/2 signaling relative to WT, but no change in Smad signaling. Losartan treatment reduces pRelA levels, but not pERK1/2 levels (n=9 per group, representative lanes shown in Figure 2G).

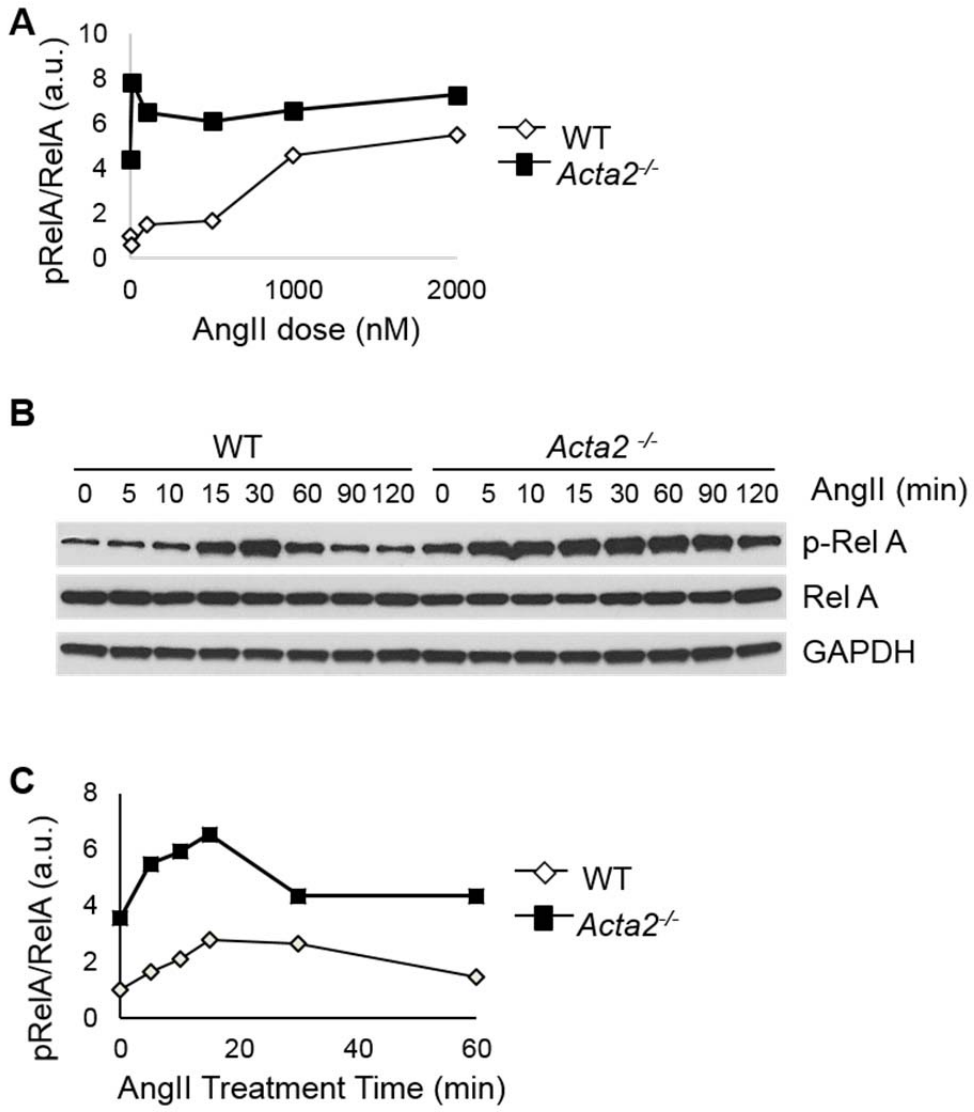

Online Figure IV Increased angiotensin sensitivity of *Acta2*$^{-/-}$ SMCs in culture (A) Quantitation of immunoblot shown in Figure 3A. *Acta2*$^{-/-}$ SMCs have increased baseline pRelA and respond to a 100-fold lower dose of exogenous AngII added to culture media than WT SMCs. (B,C) Time response curve (1000nM dose of AngII) shows that increased pRelA in *Acta2*$^{-/-}$ SMCs both occurs earlier and is more sustained than in WT SMCs. Quantified in (C).

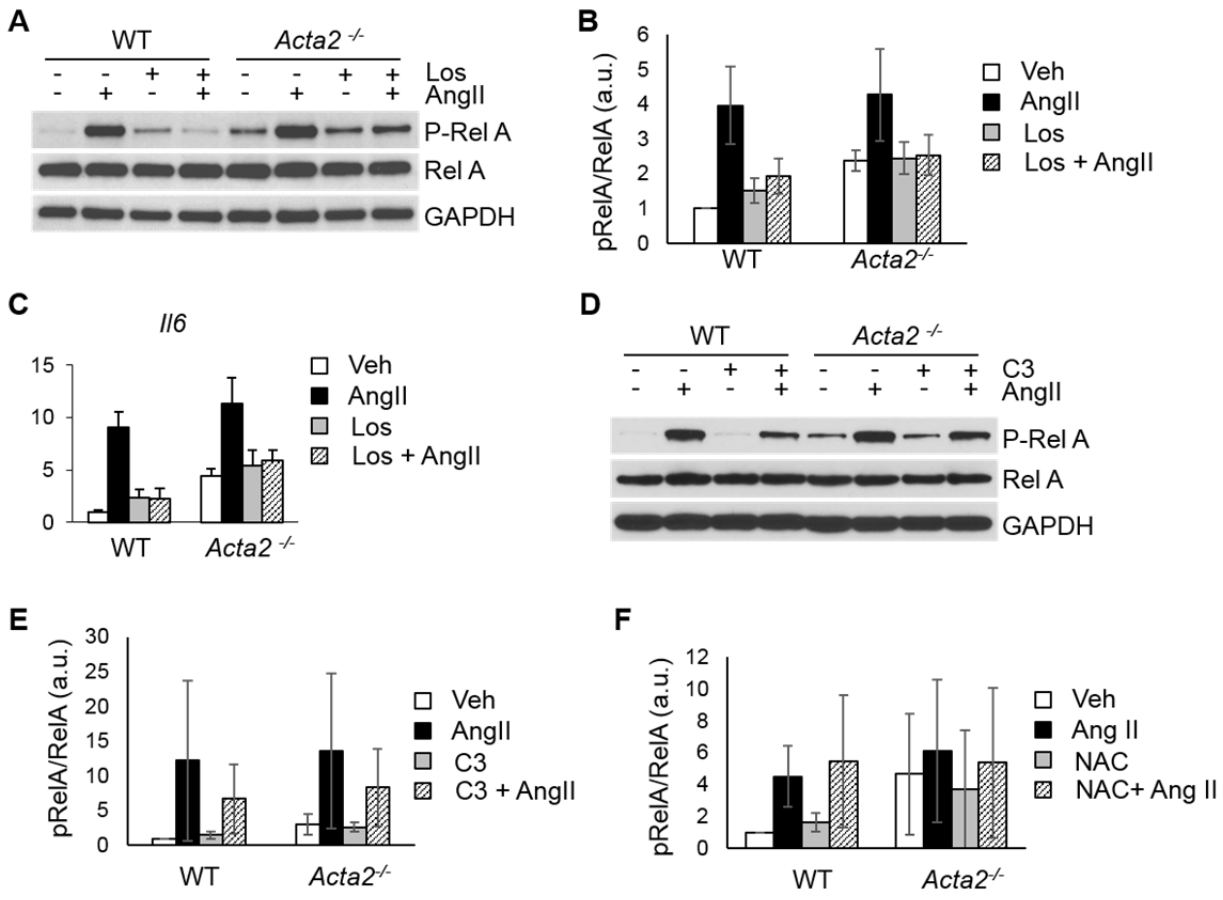

Online Figure V Losartan reduces increased angiotensin sensitivity of *Acta2*$^{-/-}$ SMCs in culture (A,B) Losartan co-treatment blocks the exogenous-AngII-induced increase in pRelA in both WT and *Acta2*$^{-/-}$ SMCs, but not the baseline increase in *Acta2*$^{-/-}$ SMCs. Quantified in (B). (C) *Il6* mRNA levels are increased in *Acta2*$^{-/-}$ SMCs, and losartan blocks the exogenous-AngII-induced increase in *Il6* levels but not the baseline increase. (D,E) Co-treatment with C3, a blocker of Rho activation, blocks the exogenous-AngII-induced increase in pRelA in both WT and *Acta2*$^{-/-}$ SMCs, but not the baseline increase in *Acta2*$^{-/-}$ SMCs. Quantified in (E). (F) Quantification of blot shown in Figure 3C. NAC co-treatment blocks both the exogenous AngII-induced increase in pRelA in both WT and *Acta2*$^{-/-}$ SMCs and the baseline increase in *Acta2*$^{-/-}$ SMCs. For all relevant panels, quantitation is based on three independent experiments, and results are presented with pRelA normalized to RelA levels.

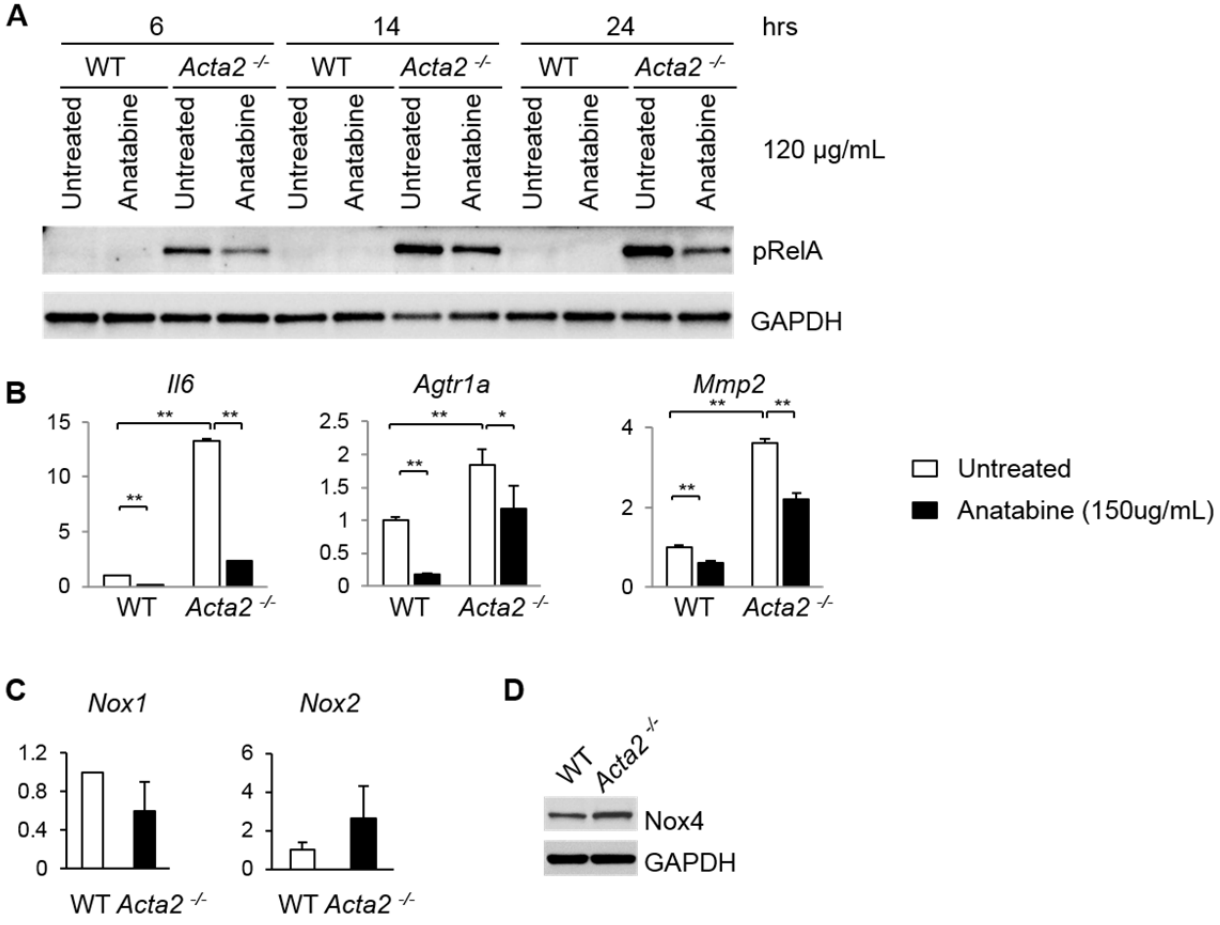

Online Figure VI Increased ROS and NF-κB signaling drive angiotensin sensitivity in *Acta2*$^{-/-}$ SMCs (A,B) Treatment with the NF-κB inhibitor anatabine (150ug/mL) for 12 hours decreases phospho-RelA (A) and reduces expression of *Il6, Agtr1a*, and *Mmp2* (B) in *Acta2*$^{-/-}$ SMCs. (C) *Acta2*$^{-/-}$ SMCs show no change in expression of *Nox1* or *Nox2*. (D) *Acta2*$^{-/-}$ SMCs have increased Nox4 protein levels.

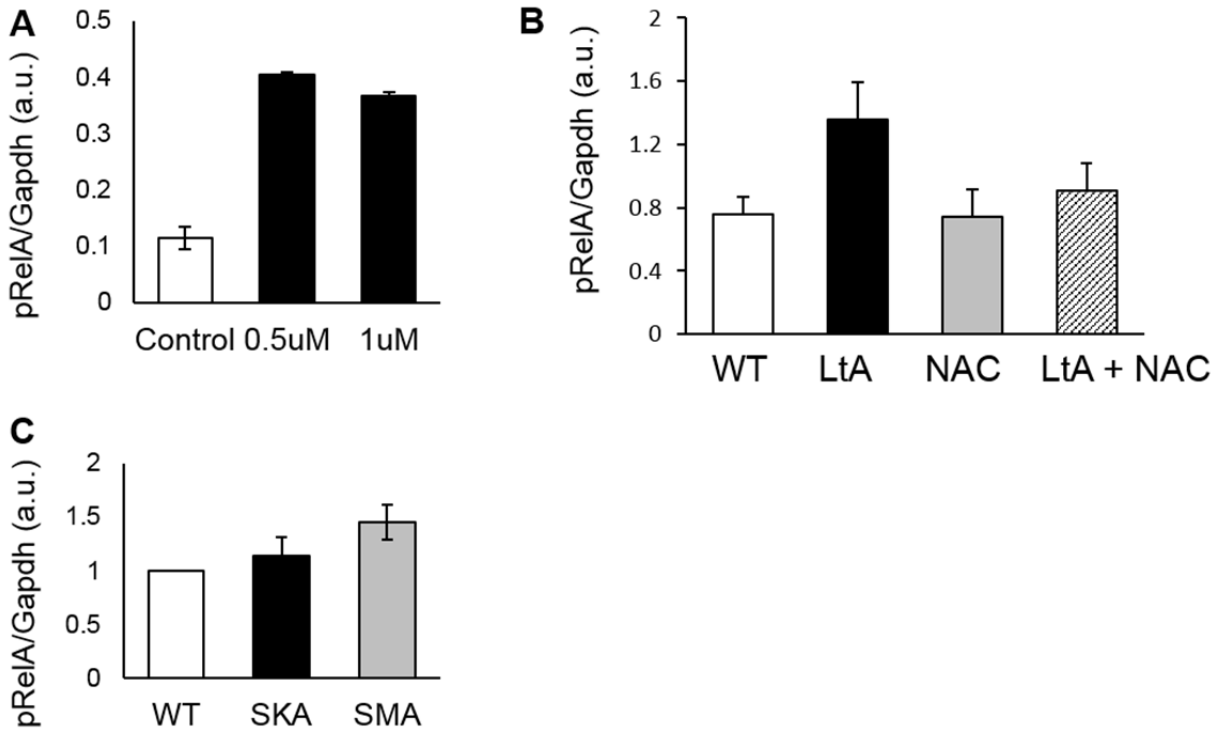

Online Figure VII Increased pRelA with disruption of SM α-actin (A) Quantitation of immunoblot shown in Figure 5B. Treatment with latrunculin increases pRelA levels. Results are shown as pRelA normalized to Gapdh. (B) Quantitation of immunoblot shown in Figure 5C. Latrunculin (LtA) was given for 24hr at 0.5uM concentration. NAC was given for 12 hours at 5mM concentration. (C) Quantitation of immunoblot shown in Figure 5E. Treatment with SMA-fp peptide but not SKA-fp peptide increases pRelA. Results are shown as pRelA normalized to Gapdh and represent five independent experiments.

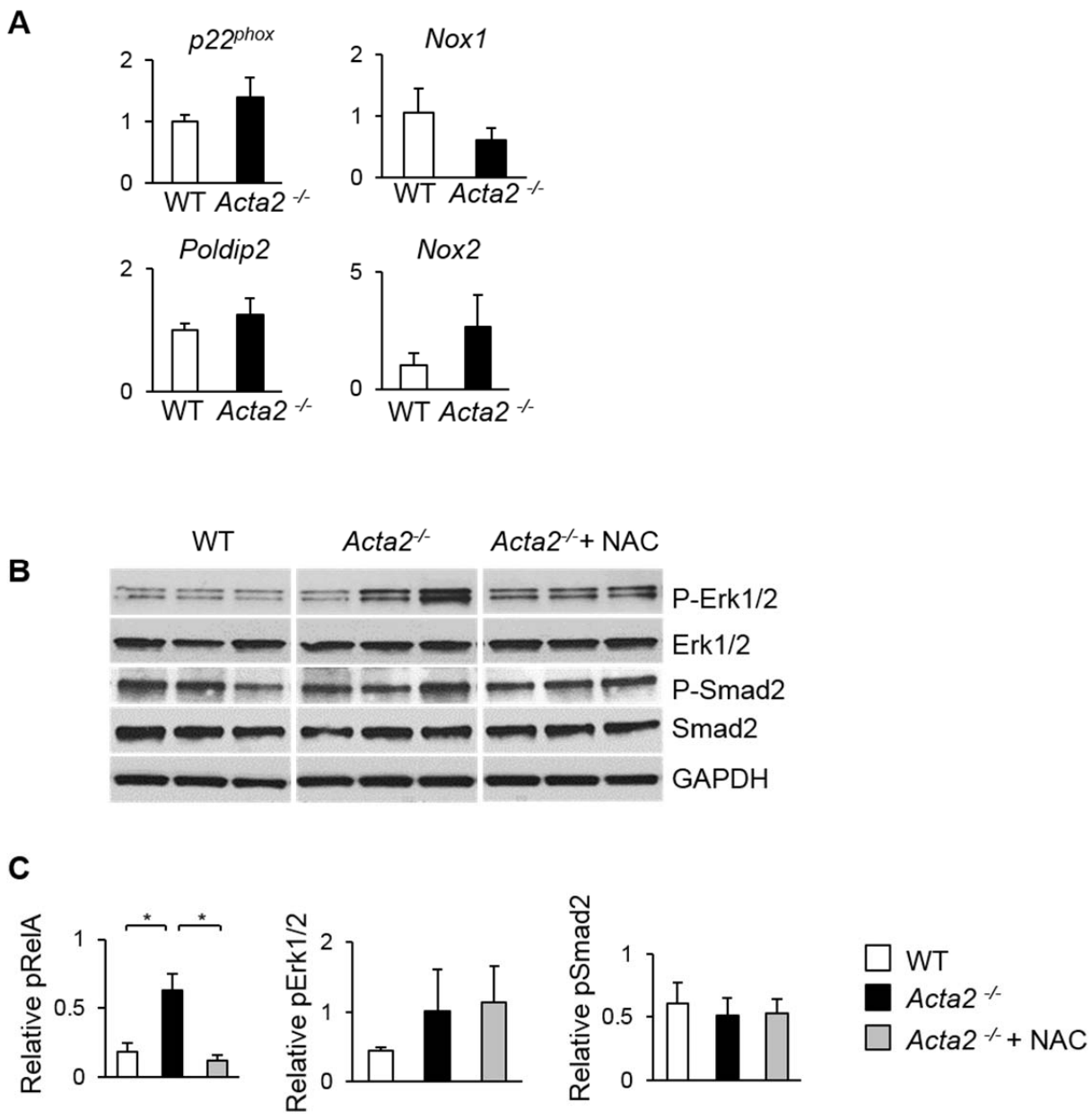

Online Figure VIII NAC treatment effectively blocks pRelA but not pERK signaling in *Acta2*$^{-/-}$ aortas (A) There is no change in expression of NADPH oxidase subunits other than *Nox4* (shown in Figure 6C) in *Acta2*$^{-/-}$ aortas. (B) Immunoblot shows increased pERK in *Acta2*$^{-/-}$ aortas which is not blocked by treatment with NAC. pSmad2 is not increased in *Acta2*$^{-/-}$ aortas. (C) Quantitation of immunoblot in Figure 6C and in (B) above. Five animals per group were

analyzed for the quantitations (three shown in the figures), and results are presented as phospho-protein normalized to total-protein (e.g. pRelA normalized to RelA).

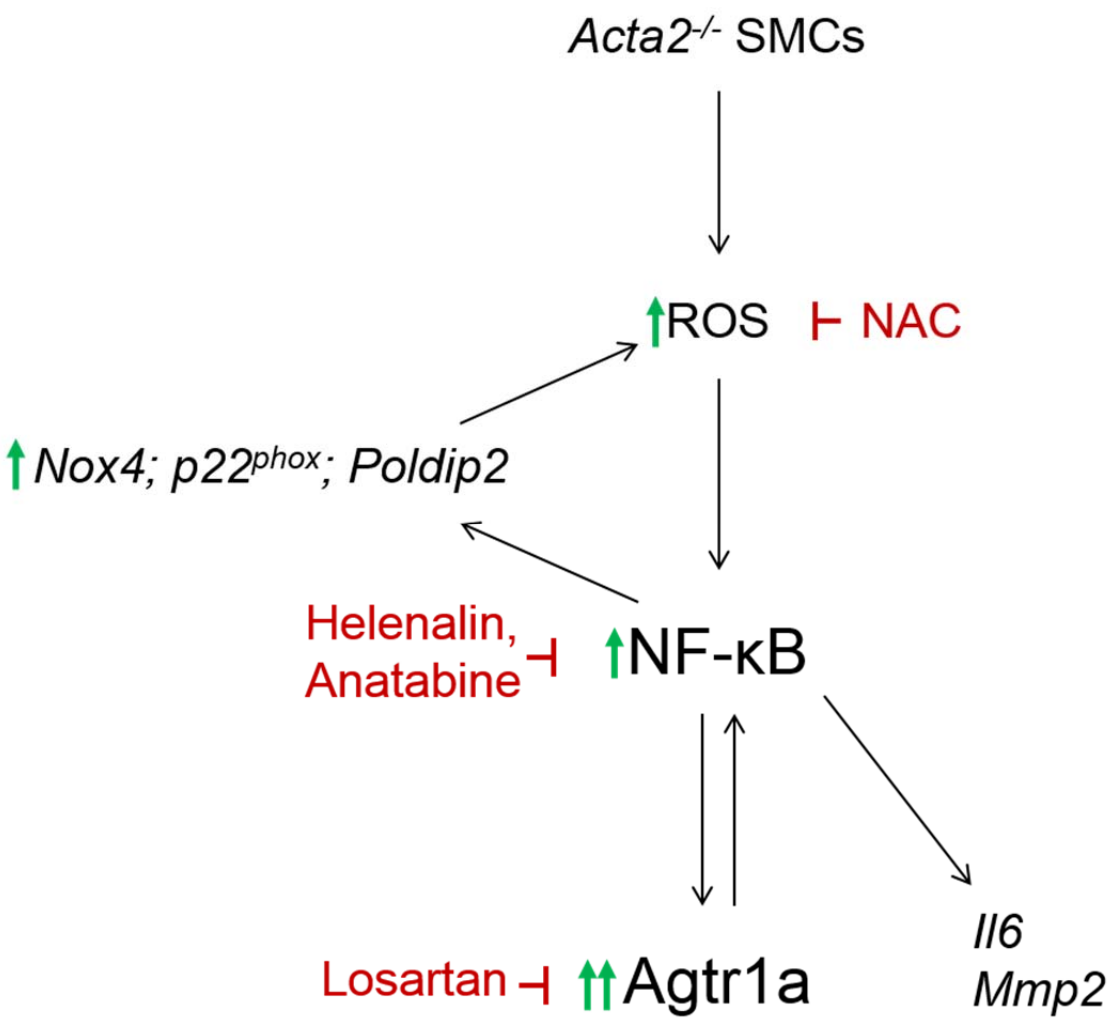

Online Figure IX Model of dysregulated signaling in Acta2$^{-/-}$ SMCs A model showing the feedback loop linking reactive oxygen species with angiotensin signaling in *Acta2*$^{-/-}$ SMCs. Note that *in vivo*, AngII is present, further activating the Agtr1a and driving both NF-κB and ROS.

Antigen	Secondary Needed	Application	Company	Catalog #
SM-MHC	Rb	WB	Biomedical Technologies INC	BT-562
SM22α	Rb	WB	Abcam	ab14106
SM α-actin	Ms	WB, IF	Sigma	A2547
Pan-actin	Rb	WB	Cytoskeleton	AAN01
Gapdh	Rb	WB	Cell Signaling	2118s
Nox4	Rb	WB	Abcam	ab109225
pRelA	Rb	WB	Cell Signaling	3033s
RelA	Rb	WB	Cell Signaling	3034s
pERK1/2	Rb	WB	Cell Signaling	9101s
ERK1/2	Rb	WB	Cell Signaling	9102s
pSmad2	Rb	WB	Invitrogen	400800
pSmad3	Rb	WB	Cell Signaling	9520s
Smad2	Rb	WB	Cell Signaling	5339s
Calponin	Rb	WB	Abcam	ab46794

Online Table I shows the antibodies used in preparation of this manuscript

Gene name	Forward primer (5'-3')	Reverse primer (5'-3')
Agt	cgagtgggagaggttctcaatag	gacgtggtcggctgttcct
Ren	ggatcagggagagtcaaaggttt	tcacagtgattccacccacagt
Ace	gggcattgacctagagactgatg	cttgggctgtccggtcata
Enpep	ccccatgatagagacgtactttca	cctgccatcccagcaaatc
Agtr1a	actcacagcaaccctccaag	ctcagacactgttcaaaatgcac
Agtr1b	cgccagcagcactgtaga	ggaggggtgaattcaaaa
At2	ccctctctgggcaacctattact	atcgacactcatgcaggtaataaaaa
Poldip2	gtatgagacgggacagctatttctcca	ctgacatagtccaagcctgggatg
Nox1	catccagtctccaaacatgacag	tgcaactccccttatggtcatc
Nox2	caggaacctcactttccataagatg	aacgttgaagagatgtgcaattgt
Nox4	ctggtctgacgggtgtctgcatggtg	ctccgcacaataaaggcacaaaggtccag
$p22^{phox}$	agatcgagtgggccatgtgggccaacgaac	cttgggtttaggctcaatgggagtccactgctca
Gapdh	caaaatggtgaaggtcggtgtg	tgatgttagtggggtctcgctc

Online Table II shows the qPCR primers used for SYBR green assays in this manuscript